Helena NOWAKOWSKA[1], Marcin LACKOWSKI[1] Jerzy MIZERACZYK[2]

The Szewalski Institute of Fluid-Flow Machinery, Polish Academy of Sciences (1), Gdynia Maritime University (2)

doi:10.15199/48.2016.08.04

Modelling of electrohydrodynamic (EHD) flow in a cylindrical precipitator with eccentric wire electrode

Abstract. *Results of calculations of EHD flow in precipitator with external tube electrode and internal wire electrode, which axes are slightly offset are presented. A set of coupled differential equations is numerically solved and 2D distributions of charge density, potential and induced flow velocity patterns are obtained. It is shown that a jet forms along the offset line and two vortices symmetrical to this line are generated.*

Streszczenie. *Przedstawiono wyniki obliczeń przepływu EHD w układzie obejmującym cylindryczną elektrodę zewnętrzną i wewnętrzną elektrodę drutową, których osie są nieznacznie przesunięte. Rozwiązano numerycznie układ sprzężonych równań różniczkowych i otrzymano dwuwymiarowe rozkłady gęstości ładunku, potencjału oraz indukowanego pola przepływu. Pokazano, ze w takim układzie tworzy się strumień gazu wzdłuż kierunku przesunięcia oraz dwa symetryczne wiry. (**Modelowanie przepływu EHD w cylindrycznym elektrofiltrze z przesuniętą elektrodą drutową**).*

Keywords: EHD flow, electrostatic precipitator, numerical modelling.
Słowa kluczowe: przepływ elektrohydrodynamiczny, elektrofiltr, modelowanie numeryczne.

Introduction

Corona discharge is a gas discharge generated in a region close to a high-potential electrode with a small curvature radius. Ions produced in the discharge move in the electric field and their collisions with neutral molecules cause a movement of electrically neutral gas. This phenomenon called an EHD flow finds applications for example in electrostatic precipitators to clean contaminated air from dust particles, in small-size cooling devices to enhance heat transfer or in actuators to reduce drag coefficients [1]. Much research, both experimental and theoretical, has been done to understand these phenomena and optimise devices that utilize them. However, due to complexity of the problem there are still a lot of issues that are not fully understood even in a simple geometry such as a cylindrical precipitator consisting of a circular tube (collecting electrode) with a wire (high-potential) electrode inside.

It was shown recently [2] that the EHD flow observed experimentally in such a system [3] does not occur when the electrode arrangement is perfectly symmetrical; however even a small degree of asymmetry, which is always present in real systems, can induce such flow. Numerical calculations presented in [2] showed that the eccentricity ε, defined as the ratio of the displacement of the wire electrode d to the tube radius r_t (Fig. 1) even as low as ε = 0.5% can cause a noticeably flow. These calculations were performed using (i) method of characteristics (MOC) as simplification to find both the charge density and electric potential and (ii) FLUENT software to find the gas flow. It was assumed that the ionization zone thickness is zero, which is justified when the radius of the wire electrode is much smaller than the radius of the collecting electrode. Additionally, it was assumed that the gas flow does not influence the charge density or electric potential.

We performed calculations for similar conditions as in [2] but using COMSOL Multiphysics software [4], which applies a finite element method to solve partially differential equations. We assumed that the system is axially uniform and there is no axial gas flow and solved a set of fully coupled equations for the following variables: the charge density, electric potential, gas velocity and pressure. To determine the boundary condition for the charge density on the wire electrode we applied Kaptsov's assumption [5], which states that after a corona is formed, when the electric potential is above the onset level, the electric field strength on the wire electrode remains constant even if the electric potential changes.

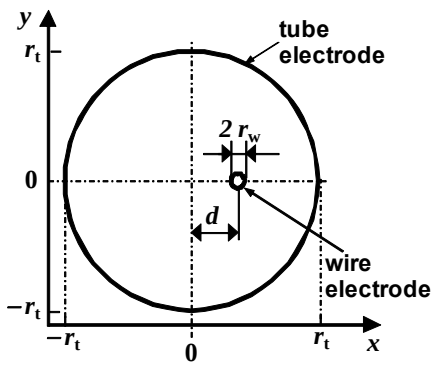

Fig.1. Cross section of a cylindrical precipitator with eccentric wire electrode.

Numerical model

Numerical model used in the present paper is based on that presented in [6], where also COMSOL software was used to model EHD flow in a wire-to-grid channel. Stationary EHD flow in air is described by the following set of coupled differential equations.

The space charge distribution can be found from the ion current conservation equation:

$$\nabla \cdot \mathbf{J} = 0 \,, \tag{1}$$

where the ion current density $\mathbf{J}$ is the sum of ion diffusion, conduction and convection currents. It can be determined from:

$$\mathbf{J} = -D\nabla q + q\mu_E \mathbf{E} + \mathbf{u}q \,, \tag{2}$$

where: q – the space charge density, D – ion diffusion coefficient, $\mathbf{u}$ – gas velocity, μ_E – ion mobility in the electric field, $\mathbf{E}$ – electric field connected with the electric potential V via the formula

$$\mathbf{E} = -\nabla V \,. \tag{3}$$

The electric potential is governed by Poisson's equation, which takes into account the space charge distribution:

$$\nabla^2 V = -q/\varepsilon_0 \,, \tag{4}$$

where: ε_0 – the electric permittivity of vacuum.

The gas flow is described by Navier-Stokes equations for laminar incompressible flow:

(5) $$\rho(\mathbf{u}\cdot\nabla)\mathbf{u} = -\nabla p + \mu\nabla^2\mathbf{u} + \mathbf{F},$$

(6) $$\nabla\cdot\mathbf{u} = 0,$$

where: p – gas pressure, ρ – air density, μ – air dynamic viscosity, $\mathbf{F}$ – the body force acting on the gas, which is equal to:

(7) $$\mathbf{F} = -q\nabla V.$$

The boundary conditions for the equations are as follows. For Navier-Stokes equations 'no-slip' ($\mathbf{u}$ = 0) condition is applied on both electrodes. The electric potential is set to zero on the collecting electrode. The electric field on the wire electrode is chosen to be equal to E_P resulting from the Peek's formula [7]:

(8) $$E_\mathrm{P} = 31.02\cdot 10^5 \delta\left(1+\frac{0.308}{\sqrt{r_\mathrm{w}\delta}}\right),$$

where: r_w – the wire electrode radius and δ is the relative air density expressed as [7]

(9) $$\delta = \frac{293}{T}\frac{p}{101325},$$

with T being the gas temperature. All values in equations (8) and (9) are in SI units.

For the space charge equation, zero diffusive flux condition ($-D\nabla q$ = 0) was chosen on the collecting electrode. The space charge on the wire electrode, q_0, was adjusted to obtain the electric potential on this electrode equal to V_0, the voltage applied to the wire electrode.

We used the following physics interfaces of the main COMSOL Module: Electrostatic, Laminar Flow and Transport of Diluted Species (modified to account for migration in the electric field). We tested several meshes to assure that the results do not depend on the chosen one. The chosen mesh consists of about 2.5x10^5 elements and is refined to about 1.7 μm in the vicinity of the wire. To verify our calculations we compared our 2D results with numerical calculations presented in [8] performed using COMSOL for axisymmetric 1D case for the tube and wire radii 17 mm and 0.15 mm, respectively, and obtained perfect agreement.

Results

The calculations were performed in 2D geometry for the tube radius r_t = 12.7 mm, r_w = 0.127 mm and three values of wire electrode potential V_0: 7.5 kV, 9.75 kV and 10.5 kV. The following parameters were used: T = 300 K, p =101325 Pa, D = 2.6x10^{-6} m^2/s, μ_E = 1x10^{-4} m^2/(V·s), ρ = 1.225 kg/m^3, μ = 18.27 μPa·s.

In the first step, we determined distributions of the electric potential and charge density for axisymmetric case (ε = 0%) and compared them with results obtained using analytical formulas derived in [9]. The comparison of the charge density distributions along r (the distance from the wire electrode centre) is shown in Fig. 2, where results from [2] are also presented. Excellent agreement between our and analytical results is seen. The results from [2] differ significantly. They obtained that the charge density drops to zero on the collecting electrode. Such result (if it is not an error in their normalization description) violates eq. (1) and is inconsistent with the experiment because it means that the density of the electric current reaching the collecting electrode, which taking into account the imposed boundary conditions is

(10) $$\mathbf{J} = q\mu_E\mathbf{E},$$

drops to zero as well.

Agreement between our results and analytical ones for other values of V_0 and for the potential distribution $V(r)$, is also excellent.

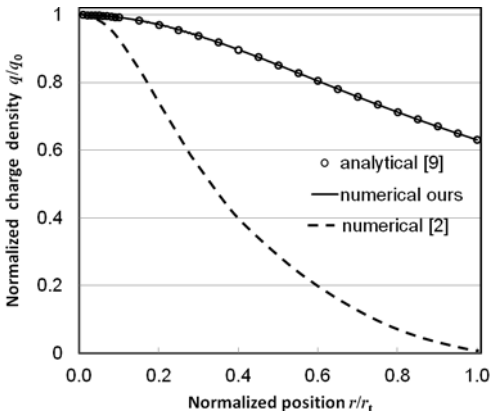

Fig.2. Normalized charge density vs. normalized position along the radius, ε = 0%.

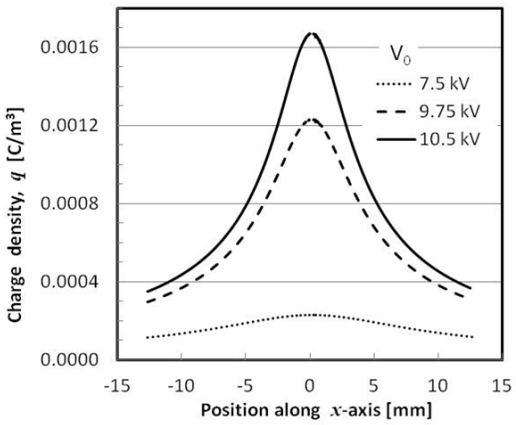

Fig.3. Charge density distributions along the x-axis for three electric potential values, ε = 1%.

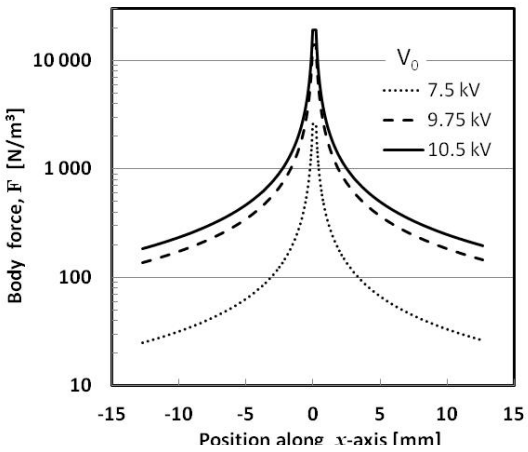

Fig.4. Body force density distributions along the x-axis for three electric potential values, ε=1%.

The charge density and the body force along x-axis for y = 0 (Fig. 1) obtained for ε = 1% and three values of the wire electrode potential are presented in Fig. 3 and 4,

respectively. For such a small eccentricity the distributions are almost symmetrical with respect to the wire axis. The body force is maximal at the wire axis and drops almost as $1/r$. Its value for x = 12.7 mm is about 5% grater than for x = –12.7 mm. This small asymmetry induces the gas flow.

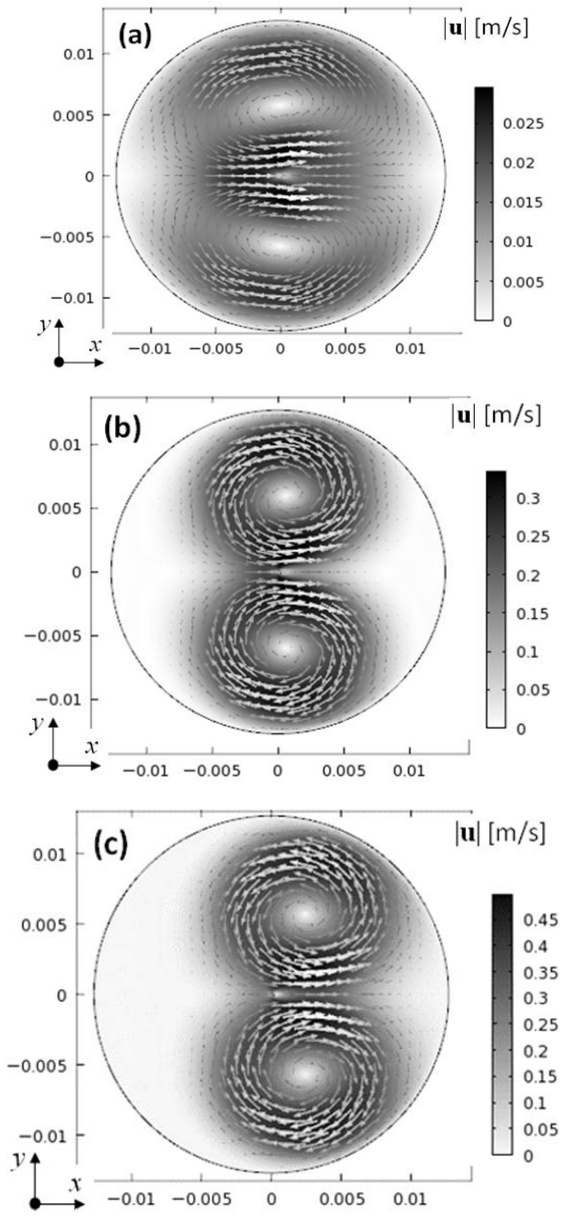

Fig.5. Velocity fields |**u**| and velocity vectors for different values of V_0, a) 7.5 kV, b) 9.75 kV, c) 10.5 kV. The scale of the axes is in [m].

Patterns of the flow are shown in Fig. 5. It is seen that a jet forms along the x-axis and two vortices form above and below the symmetry plane. When the voltage applied to the wire increases, the vortices' centres move in +x direction and the maximum gas velocity increases, reaching 0.5 m/s for V_0 = 10.5 kV. The velocities of the gas along y = 0 line are shown in Fig. 6, where two local maxima are seen for each V_0. The maximal velocity on this line is 0.35 m/s forV_0 = 10.5 kV and this maximum is located on the side of positive x's, whereas for lower potentials the higher maximum is for negative x's.

The values of the velocity presented in Fig. 5 and 6 seem reasonable when comparing them with experimental values from [10], where the dust particles maximum velocity measured using PIV method for similar conditions but ε = 20% was about 1.6 m/s.

The characteristic velocities u_e calculated from the formula

$$u_e = \sqrt{q_0 V_0 / \rho} \tag{10}$$

are 1.2 m/s, 3.2 m/s and 3.8 m/s, whereas the values of EHD Reynolds number Re_{EHD} calculated from

$$\mathrm{Re}_{EHD} = \rho u_e r_t / \mu_E \tag{11}$$

are 1000, 2665 and 3222 for the applied electrode voltage V_0 equal to 7.5 kV, 9.75 kV and 10.5 kV, respectively.

The values of velocity shown in Fig. 5 and 6 are smaller than those arising from the data presented in [2], where absolute values of velocity are not given directly, but in terms of u_e and Re_{EHD}. EHD Reynolds number obtained there for V_0 = 10.5 kV is 8145. This number allows us to determine from (11) their characteristic velocity u_e as 9.6 m/s and estimate the maximal velocity in jet as about 30 m/s.

The vortices in our case (Fig. 5) are shifted to the right but not so much as in [2], where they occupy virtually only the right side of the tube. Again, our patterns are more similar to experimentally obtained ones for dust particles from [10].

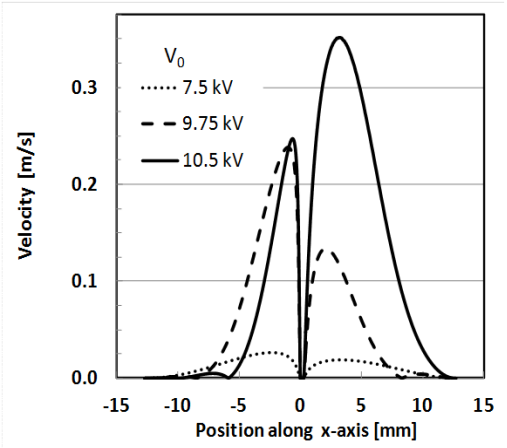

Fig.6. The gas velocity along the x-axis for three applied voltage values.

Summary and conclusion

The numerical analysis of EHD flow in cylindrical precipitator with wire electrode confirmed that eccentricity of order 1% can induce a noticeable gas flow. Except of a jet that forms along the x-axis also two vortices are generated above and below the symmetry plane. Our numerically obtained results differ from that obtained in [2], where different assumptions and numerical methods are applied. The comparison of the results shows that the final results are sensitive to the chosen assumptions and used simplifications. This means that further study and comparison with the experiment is needed to fully understand the phenomenon.

This research has been supported by National Centre of Research and Development in the framework of Contract SP/E/4/65786/10 Strategic Research Programme Advanced Technologies for Energy Generation, Research Task No. 4.

Authors: *dr inż. Helena Nowakowska, dr inż. Marcin Lackowski, Instytut Maszyn Przepływowych PAN, ul. Fiszera 14, 80-231 Gdańsk, E-mail: helena@imp.gda.pl; mala@imp.gda.pl; prof. dr hab. inż. Jerzy Mizeraczyk, Akademia Morska, Katedra Elektroniki Morskiej, ul. Morska 81-87, 81-225 Gdynia, E-mail: jmiz@imp.gda.pl*

REFERENCES

[1] Fylladitakis E.D., Theodoridis M.P., Moronis A.X., Review on the history, research, and applications of electrohydrodynamics *IEEE T Plasma Sci*, 42 (2014), No. 2, 358-375

[2] Lakeh R.B., Molki M., Patterns of airflow in circular tubes caused by a corona jet with concentric and eccentric wire electrodes. *J. Fluids Eng*., 132 (2010), 081201

[3] Niewulis A., Podliński J., Berendt A., Mizeraczyk J., EHD Flow Measured by 2D PIV in a Narrow Electrostatic Precipitator with Longitudinal Wire Electrode, *Przegląd Elektrotechniczny*, 88 (2012) 164-167

[4] www.comsol.com

[5] Kaptzov N., Elektricheskiye yavleniya v gazakh i vacuume OGIZ (1947), 587-630

[6] Jewell-Larsen N.E., Karpov, S.V., Krichtafovitch I. A., Jayanty V., Hsu C.P. and Mamishev A.V., Modeling of corona-induced electrohydrodynamic flow with COMSOL multiphysics, *Proc. ESA Annual Meeting on Electrostatics* (2008) Paper E, 1

[7] Peek J.F.W., Dielectric Phenomenon in High Voltage Engineering, McGraw-Hill, Book Company (1915)

[8] Benamar B., Favre E., Donnot A., Rigo M.O., Finite element solution for ionized fields in DC electrostatic precipitator. *Proceedings of the COMSOL Users Conference* (2007) 23-24

[9] Janischewskyj W., Gela G., Finite element solution for electric fields of coronating dc transmission lines, *IEEE Trans. Power Appar. Syst*., 98 (1979) 1000-1012

[10] Niewulis A., Podliński J., Berendt A., Mizeraczyk J., Influence of Electrode Geometric Arrangement on the Operation of Narrow Circular Electrostatic Precipitator, *Int. Journal of Plasma Environmental Science & Technology*, 8 (2014), No. 1, 60-71